2020-10-10

Highly polarised gamma photons from electron-laser collisions

Tang, S

10.1016/j.physletb.2020.135701
Physics Letters B
Elsevier BV

Physics Letters B 809 (2020) 135701

Contents lists available at ScienceDirect

Physics Letters B

www.elsevier.com/locate/physletb

Highly polarised gamma photons from electron-laser collisions

S. Tang [a,*], B. King [a], H. Hu [b]

[a] Centre for Mathematical Sciences, University of Plymouth, Plymouth, PL4 8AA, United Kingdom
[b] Hypervelocity Aerodynamics Institute, China Aerodynamics Research and Development Center, 621000 Mianyang, Sichuan, China

ARTICLE INFO

Article history:
Received 13 May 2020
Received in revised form 10 August 2020
Accepted 13 August 2020
Available online 19 August 2020
Editor: A. Ringwald

ABSTRACT

We detail a method to produce a GeV-photon source with polarisation degree exceeding 91% and 78% (corresponding to a 96% and 89% fraction of the photons) for linear and circular polarised photons respectively and with a brilliance of the order of 10^{21} photons/(s mm^2 mrad^2 0.1% BW). Using currently available multi-GeV electron bunches and laser pulses of moderately relativistic intensities, we show how the weakly nonlinear regime can produce photons polarised mainly parallel to the laser field. We demonstrate the robustness of this scheme by considering electron bunches of various emissivities colliding with linearly and circularly-polarised laser pulses at a range of angles.

1. Introduction

When an accelerated electron bunch scatters off a laser pulse of sufficient intensity, photons are produced in a series of harmonics corresponding to the number of absorbed laser photons. As the intensity of the pulse is increased, there is predicted to be a transition from the perturbative *multi-photon* regime, where spectra are well-approximated by considering just the lowest harmonics, to the *small-coupling non-perturbative* regime where all orders of harmonics can contribute equally. Experiments such as LUXE at DESY [1] and E320 at FACET-II [2] are planned in the near future to combine electron bunches of order 10 GeV with laser pulses of intensity parameter $\xi \sim O(1)$ to measure, for the first time, the transition from the multi-photon to the non-perturbative regime of quantum electrodynamics (QED). They will thereby complement the landmark E144 experiment, which measured processes in the multi-photon regime two decades ago [3–5]. The measurement and characterisation of the non-perturbative regime is highly relevant to the design and analysis of experimental campaigns planned at the next generation of high power laser facilities such as ELI-Beamlines, ELI-NP [6], EP-OPAL and SEL [7], which will realise this regime in intense laser-plasma interactions.

Photon polarisation is an important experimental observable, which was central to measurements providing the first evidence of real photon-photon scattering (vacuum birefringence) from an isolated neutron star [8], and measuring the polarisation of X-ray sources is a key part of the future Imaging X-ray Polarimetry Explorer (IXPE) [9]. Having access to a highly-polarised source of photons has also been shown to significantly reduce the experimental demands required to provide the first experimental measurement of real photon-photon scattering using lasers in the lab [10–12]. The decay of a photon into an electron-positron pair in an intense electromagnetic field, which is believed to play an important role in the evolution of the magnetospheres of some neutron stars [13], and a key observable in the LUXE and E320 experiments, can also be considerably enhanced by using a highly-polarised photon source [14]. Using pair spectroscopy [15], the polarisation purity can form a useful further interrogation of high-intensity QED. Furthermore, polarised photons also find application in e.g. the study of nuclear structure via photonuclear reactions [16].

In this letter, we propose a robust scheme to generate brilliant and highly-polarised GeV γ-rays collimated by colliding an electron bunch nearly head-on with a laser pulse of intermediate intensity. By considering an electron bunch with a divergence of 0.2 mrad [17], the photon source is predicted to have a polarisation degree of around 91% and 78% for linear and circular polarisation respectively, and a brilliance of up to 10^{21} photons s^{-1} mm^{-2} mrad^{-2} 0.1% BW. Because our scheme exploits the harmonic and angular structure of the spectrum, it is beyond analyses based on numerical simulations that employ the locally-constant-field approximation [18–22]. For this reason, the predicted brilliance of our scheme is orders of magnitude higher than hitherto conceived for a polarised hard gamma source [23]. Furthermore, as we will show, our scheme is robust and does not rely upon fine-tuning of experimental parameters.

* Corresponding author.
E-mail addresses: suo.tang@plymouth.ac.uk (S. Tang), b.king@plymouth.ac.uk (B. King).

https://doi.org/10.1016/j.physletb.2020.135701

2. Polarised NLC in plane wave backgrounds

We begin by outlining definitions used in the calculation. In an electron-laser collision, the differential probability of emitting a photon in the polarisation state ε_j with momentum k via the nonlinear Compton process [24,14], can be written as [25]

$$\frac{\mathrm{d}^3\mathsf{P}_j}{\mathrm{d}s\,\mathrm{d}\mathbf{r}^2} = \frac{\alpha}{(2\pi\eta)^2}\frac{s}{t}\int \mathrm{d}\phi\,\mathrm{d}\phi'\,\mathsf{T}_j \mathrm{e}^{\,i\int_{\phi'}^{\phi}\frac{k\cdot\pi_p(\varphi)}{m^2 t\eta}\mathrm{d}\varphi}, \tag{1}$$

where we model the laser pulse as a plane wave with wavevector $\varkappa = \varkappa^0(1,0,0,1)$, α is the fine-structure constant, $\eta = \varkappa\cdot p/m^2$, $s = \varkappa\cdot k/\varkappa\cdot p$ is the lightfront momentum fraction of the scattered photon, $t = 1-s$, ϕ (ϕ') is the laser pulse phase, $\pi_p = p - a + \varkappa(2\,p\cdot a - a^2)/\varkappa\cdot p$, $a = eA$ where A is the laser pulse vector potential, p, e and m are the electron incident momentum, absolute charge and mass respectively and T_j is a polarisation-dependent integrand defined later. $\mathbf{r} = \boldsymbol{k}^\perp/(sm)$ is the normalised photon momentum in the plane perpendicular to the laser propagation direction and relates directly to the scattering angle of the photon. For later use, we define the angles to the negative z axis, $\theta_{x,y}$, of the scattered photon in the x-z and y-z planes, via $r_{x,y} = m\eta\tan(\theta_{x,y}/2)/\varkappa^0$. The photon polarisation states are chosen to be the eigenstates of the polarisation operator in the given laser background to ensure the polarisation does not change after the photon is created. For a linearly-polarised laser pulse: $a(\phi) = m\xi\varepsilon_1\sin(\phi)f(\phi)$ where ξ and $f(\phi)$ are the laser amplitude and profile, and we use the normalised transverse states [26]:

$$\epsilon_1 = \varepsilon_1 - \frac{k\cdot\varepsilon_1}{k\cdot\varkappa}\varkappa\,, \quad \epsilon_2 = \varepsilon_2 - \frac{k\cdot\varepsilon_2}{k\cdot\varkappa}\varkappa, \tag{2}$$

where $\varepsilon_1 = (0,1,0,0)$ and $\varepsilon_2 = (0,0,1,0)$ are parallel to the laser electric and magnetic fields respectively. For a circularly-polarised background $a(\phi) = m\xi[\varepsilon_1\cos(\phi) + \varepsilon_2\sin(\phi)]f(\phi)$,[1] we use $\epsilon_\pm = (\epsilon_1 \pm i\epsilon_2)/\sqrt{2}$, where the sign $+$ ($-$) denotes the left-hand (right-hand) rotation of the polarisation. We will generally refer to ϵ_1/ϵ_+ (ϵ_2/ϵ_-) states as *E/L-polarised* (*B/R-polarised*) and as being parallel (perpendicular) to the field, even though, in general, the photon is not emitted head-on with the laser pulse, but instead at a small opening angle and so its polarisation direction is not exactly aligned with the field. We find:

$$\mathsf{T}_j = \frac{s^2}{8t}\Delta + w_j(\phi)\cdot w_j(\phi'), \tag{3a}$$

$$\mathsf{T}_\pm = \frac{s^2}{8t}\Delta + \frac{1}{2}\boldsymbol{w}(\phi)\cdot\boldsymbol{w}(\phi') \pm i f_t\,\boldsymbol{w}(\phi)\times\boldsymbol{w}(\phi'), \tag{3b}$$

where $\boldsymbol{w}(\phi) = (\mathbf{r} - \boldsymbol{p}^\perp/m)R(\phi) + \boldsymbol{a}^\perp(\phi)/m$, $\Delta = [a(\phi) - a(\phi')]^2/m^2$, $f_t = (1+t^2)/(4t)$ and $R(\phi) = 1 - k\cdot\pi(\phi)/k\cdot p$ is the regulator (see e.g. [28] for details).

In Eq. (3), we see the polarisation-dependent part of the scattering probability for a linearly polarised background T_j and for a circularly-polarised background $\mathsf{T}_\pm$ is quite different. This dependence can lead to a significant difference in the energy and angular distribution of the scattered polarised photons. We use the *polarisation degree* $\mathcal{P}$, which varies from -100% to 100%, and signifies the asymmetry in the polarisation mix of emitted photons. The E-polarised (L-polarised) states are used to define positive asymmetry: $\mathcal{P} = (\mathsf{P}_1 - \mathsf{P}_2)/(\mathsf{P}_1 + \mathsf{P}_2)$ ($\mathcal{P} = (\mathsf{P}_+ - \mathsf{P}_-)/(\mathsf{P}_+ + \mathsf{P}_-)$) for a linearly (circularly) polarised background. As an example in Fig. 1, we consider[2] the head-on collision between a 10 GeV ($\eta = 0.095$) electron and a 26.7 fs (8-cycle) laser pulse with intermediate intensity $\xi = 0.5$. The importance of quantum and nonlinear contributions in this parameter regime is discussed in Appendix A. Fig. 1(a) shows the different behaviour of the polarised energy spectra in the linearly and circularly polarised background for different values of s. In the $s\to 0$ limit, the photons are almost unpolarised in a linearly-polarised background, whereas in a circularly-polarised background, almost all photons are R-polarised ($\mathcal{P}\to -100\%$) [27,30]. Recalling that $s\propto 1+\cos\theta_p$, where $\theta_p \approx (\theta_x^2+\theta_y^2)^{1/2}$ is the photon scattering angle with respect to the negative z-axis, we see that, although there is a source of highly polarised photons when $s\to 0$, this corresponds to: i) low energies and ii) broad angular spread. However, another source of highly-polarised photons is at higher s-values starting around the Compton edge (the end of the kinematic range of the first harmonic [31]), where in both linearly- and circularly-polarised backgrounds, the polarisation degree remains very high as shown in Fig. 1(b) and the photons are almost entirely polarised in the E/L-states. The multiple peaks in Fig. 1(b) correspond to different orders of harmonics. For a circularly-polarised background, the Compton edge is at $s = 2\eta/(2\eta+1+\xi^2)$ (for a linearly-polarised background $\xi^2\to\xi^2/2$). Furthermore, as shown in Fig. 1(c) and Fig. 1(e), the photons in the E/L-polarised states are tightly collimated with the electron's incident direction ($\vartheta_i = 0$) with an angular spread of $\sim 2\xi/\gamma_p$, where $\gamma_p \approx 2\times 10^5$ is the Lorentz factor of the initial electron, in contrast to the broader angular spread

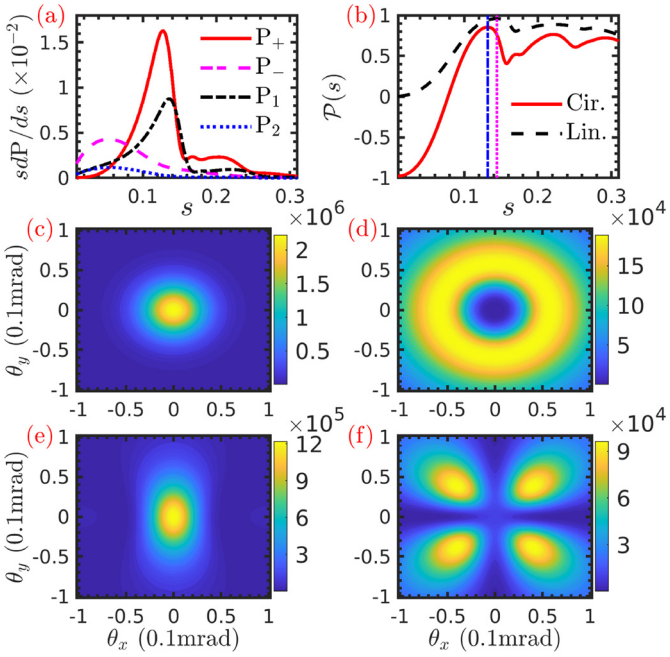

Fig. 1. Energy and angular spectra for a head-on collision of a 10 GeV ($\eta = 0.095$) electron beam with a $\xi = 0.5$, $\omega_l = 1.24$ eV, 26.7 fs (8-cycle) laser pulse with envelope $f(\phi) = \cos^2(\phi/4\sigma)$ ($|\phi| \le 2\pi\sigma$). Upper panels: (a) energy spectrum of the polarised photon $s\,d\mathsf{P}_j/ds$ and (b) polarisation degree $\mathcal{P}(s)$. Central panels: angular distribution $d^2\mathsf{P}/d\theta_x d\theta_y$ in a circularly-polarised background of L-polarised photons (c) and R-polarised photons (d). Bottom panels: angular distribution in a linearly-polarised background of E-polarised photons (e) and B-polarised photons (f). The blue (magenta) dot-dashed line in (b) denotes the Compton edge in a linearly (circularly) polarised background.

[1] The photon is right-hand polarised when the direction of the field rotation is parallel to the direction of its wavevector, otherwise the photon is left-hand polarised [27]. Therefore, the circular background is right-hand polarised, defined as propagating in z direction with a potential $a(\phi) = m\xi(\varepsilon_1 + i\varepsilon_2)e^{-i\phi}f(\phi)$. The emitted photons in the state ϵ_+/ϵ_- are left/right-hand polarised as propagating almost in $-z$ direction.

[2] To obtain our results, we evaluated Eq. (1) using a method based on writing the probability in terms of parts of the amplitude, and then numerically integrating these simpler parts before multiplying together (explained in detail in [29].

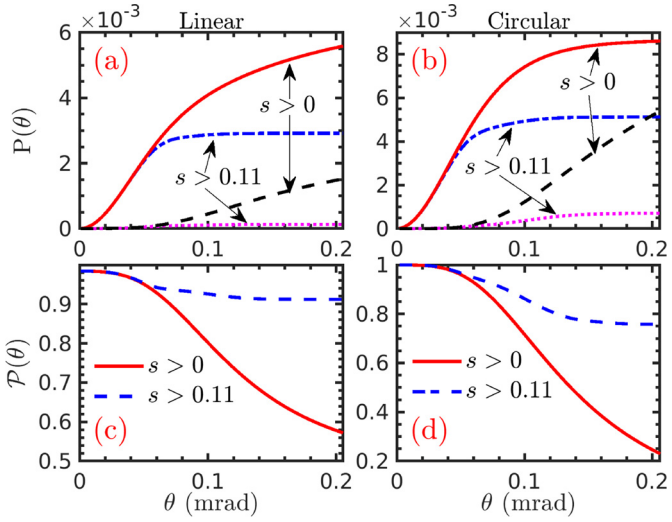

Fig. 2. Photon production probability P and polarisation degree $\mathcal{P}$ for different detector angular acceptance values, θ, for the same parameters as in Fig. 1. Left column: linearly polarised background. Right column: circularly polarised background. In (a) and (b) are the probability of a single electron scattering an E/L-polarised photon for $s > 0$ (red sold line), $s > 0.11$ (blue dot-dashed line) and probability for a B/R-polarised photon with $s > 0$ (black dashed line), $s > 0.11$ (magenta dotted line). In (c) and (d) are the polarisation degree for $s > 0$ (red sold line), $s > 0.11$ (blue dashed line).

of B/R-polarised photons shown in Fig. 1(d) and Fig. 1(f). The high E/L-polarised degree can be explained with a straightforward classical multipole expansion, since the electron recoil parameter $\chi_p = \eta\xi \approx 0.05 \ll 1$. When the laser intensity is in the intermediate range $\xi \ll 1$, $\xi \gg 1$, the (Lorentz-boosted) dipole radiation forms a large component of the Compton scattered photon distribution, with some sub-leading higher-order multipole contributions. This dipole radiation is completely polarised in the parallel state, and when the electron is highly relativistic, this radiation is emitted within a narrow opening angle parallel to the electron propagation direction at the Lorentz-boosted first harmonic energy. Multipole radiation also contributes but is suppressed directly in the higher energy region [as seen in Fig. 1(a) and Fig. 1(b)] and hence there is a high degree of E/L-polarised photons at the Compton edge. A similar explanation applies to the circularly-polarised case.[3]

3. Highly-polarised GeV γ-ray source

Based on the above observations we present a robust scheme to generate highly-polarised GeV γ-rays. Since B/R-polarised photons are more likely to be emitted at larger angles and lower energies, by applying an angular cut (through the placement of the detector) and an energy cut (through the use of an attenuating filter), the photons that remain are of a high E/L-polarisation degree.

From Eq. (1), the number of photons within the detector angular acceptance θ can be calculated:

$$\mathsf{P}_j = \int_{-\theta/2}^{\theta/2} \mathrm{d}\theta_x \int_{-\theta/2}^{\theta/2} \mathrm{d}\theta_y \int_{s_d}^{1} \mathrm{d}s \frac{\mathrm{d}r_x}{\mathrm{d}\theta_x}\frac{\mathrm{d}r_y}{\mathrm{d}\theta_y}\frac{\mathrm{d}^3\mathsf{P}_j}{\mathrm{d}s\mathrm{d}\mathbf{r}^2},$$

where s_d is a lower bound on the photon energy. In Figs. 2(a) and (b), we see that the total number of detectable photons decreases with a narrower acceptance angle θ. However, as the decrease of E/L-polarised photons is much slower than the decrease of B/R-polarised photons, the polarisation degree increases sharply by narrowing the detector acceptance angle as shown in Fig. 2(c) and (d). For a linearly polarised background (left column), the polarisation degree of the received photons increases from $\mathcal{P} \approx 58\%$ within the acceptance angle $\theta = 0.2$ mrad to 81% within $\theta = 0.1$ mrad, and increases still further to the high degree $\mathcal{P} \approx 95\%$ within $\theta = 0.05$ mrad. For the circular case (right column), the same phenomenon is presented: the polarisation degree $\mathcal{P}$ increases from 25% with $\theta = 0.2$ mrad to 72% with $\theta = 0.1$ mrad and to higher than 96% within $\theta = 0.05$ mrad. Furthermore, this high polarisation degree is carried mainly by high-energy photons because E/L-polarised photons dominate the high-energy spectrum. In Fig. 2 we also present results for high-energy photons with an energy cutoff of $s_d = 0.11$ (corresponding to 1.1 GeV), where, as shown, the number is already saturated at an acceptance $\theta \approx 0.14$ mrad, with a degree above $\mathcal{P} \approx 91\%$ ($\mathcal{P} \approx 78\%$) in a linearly-polarised (circularly-polarised) background [blue dashed line in Fig. 2(c) and (d)]. More than 90% of these high-energy photons are collimated in a much narrower angular divergence < 0.08 mrad with a degree above $\mathcal{P} \approx 92\%$ in each case, and more than 30% of these photons are above the Compton edge in Fig. 1(a) and hence from the nonlinear interaction of the electron with the laser background.

In order to obtain highly brilliant γ-rays, a bunch of energetic electrons is needed to pump the photon source. Here we consider electrons with an average energy of 10 GeV, attainable in upcoming LUXE [1] and E320 experiments [2] (all-optical set-ups using laser wakefield acceleration can achieve energies of order 5 GeV [32,17]). We calculate the effect of an electron bunch by assuming a normalised momentum distribution:

$$\rho(\boldsymbol{p}) = \frac{1}{\sqrt{2\pi^3}\sigma_\parallel\sigma_\perp^2 m^3} \exp\left[-\frac{(\boldsymbol{p}\cdot\boldsymbol{n}-\tilde{p})^2}{2\sigma_\parallel^2 m^2} - \frac{|\boldsymbol{p}-\boldsymbol{n}(\boldsymbol{p}\cdot\boldsymbol{n})|^2}{\sigma_\perp^2 m^2}\right],$$

with modulus average momentum $\tilde{p}$ and root-mean-square (rms) momentum spread in the longitudinal, $\sigma_\parallel m$, and transverse, $\sigma_\perp m$ directions, where $\boldsymbol{n} = (\sin\vartheta_i, 0, -\cos\vartheta_i)$ is the incident direction of the electron bunch. Because the wavelength of emitted photons is much smaller than the electron bunch length, we assume the emission is incoherent. We also assume that the electron bunch width is much smaller than the laser pulse focal width, as is planned for LUXE (strong laser focussing is not required as intermediate intensities are comfortably attainable by modern high-power lasers).

In Fig. 3(a) and (b), we show the angular distribution of high-energy ($s > 0.11$) E/L-polarised photons emitted by a pump electron bunch: $\sigma_\parallel = 3\%\gamma_p$ and $\sigma_\perp = 10^{-4}\gamma_p$ corresponding to a 6% rms energy spread and an angular divergence $\Theta = 0.2$ mrad, with an average momentum $\tilde{p} = \gamma_p m$ [17] incident at an angle $\vartheta_i = 100$ mrad. Because the bunch angular divergence is much larger than the angular spread $2\xi/\gamma_p$ induced by the background field, the photons are emitted in a much broader distribution of angles than the single-electron result in Fig. 1. Therefore, rather than producing a well-defined angular harmonic structure, for a bunch of electrons with a broad spread of momenta, we see that the angular harmonic structure is smoothed out. However, as in Fig. 1, we still see the dominance of the E/L-polarised photons in the high-energy region $s > 0.11$. The polarisation degree is about 91% (78%) for the linear (circular) case with acceptance $\theta = 0.2$ mrad shown in Fig. 3(c). The effect of the electron bunch is to average out the peak degree along the propagation axis, resulting in a flatter distribution which is less sensitive to the precise value of the acceptance angle. Because low-energy photons mix with higher energy photons off-axis, the maximum predicted degree is reduced, (indicated by the lines for $s > 0$ in Fig. 3(c)). To reach a higher degree, an energy filter would also have to be applied. However, we emphasise

[3] To preserve azimuthal symmetry, an expansion spherical harmonics Y_l^m would be dominated by terms with equal degree l and order m, and only Y_0^0 (which is only present in the first harmonic) has a non-zero contribution on-axis.

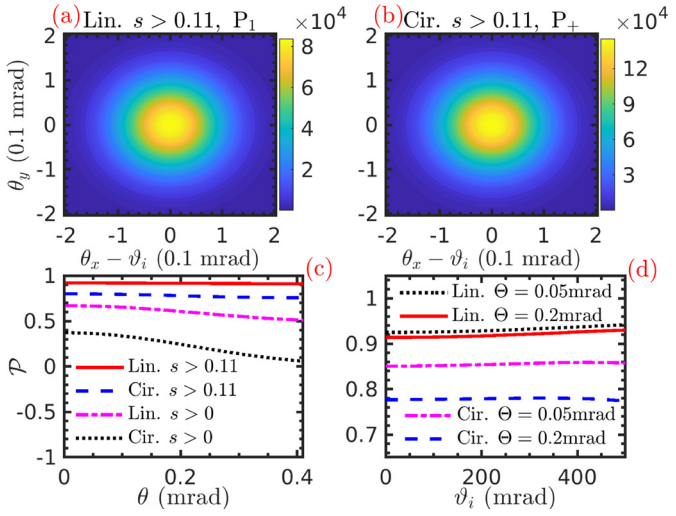

Fig. 3. For the same field parameters as in Fig. 1, with the photon detector directly along the electron propagation axis: (a) and (b) angular distribution of the high-energy ($s > 0.11$ corresponding to 1.1 GeV) E-polarised and L-polarised photons for a linearly and circularly polarised background respectively; (c) polarisation degree $\mathcal{P}$ for varying detector acceptance θ where the pump electron beam ($\Theta = 0.2$ mrad) collides with the laser pulse obliquely ($\vartheta_i = 100$ mrad); (d) polarisation degree $\mathcal{P}$ of the high-energy photons ($s > 0.11$) for varying incident angle ϑ_i of the electron beam with the divergence $\Theta = 0.2$ and 0.05 mrad respectively, where the photon detector acceptance angle is fixed equal to the beam angular divergence $\theta = \Theta$.

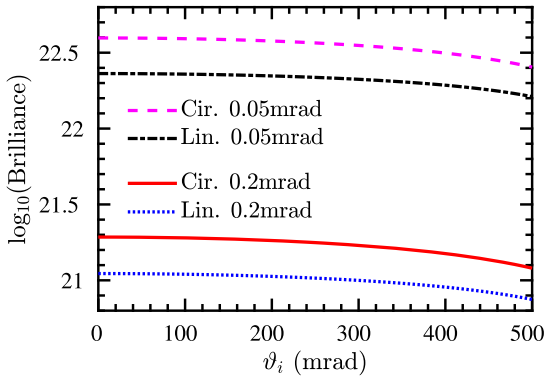

Fig. 4. Brilliance of the E/L-polarised high-energy photons ($s > 0.11$) for different incident angle ϑ_i and electron beam angular divergence $\Theta = 0.05$ mrad and 0.2 mrad. The acceptance angle of the detector is set to $\theta = \Theta$. The field parameters are the same as in Fig. 1. The electron bunch has a mean energy of 10 GeV and a root-mean-square energy spread of 6%. The photon detector is set downstream along the bunch propagation direction.

that for the application of the γ-rays to measuring vacuum birefringence and generating spin-polarised particle beams, an energy cut is unnecessary as high-energy photons naturally scatter with a higher probability than low-energy photons and hence the photons that participate in the process naturally have a higher polarisation degree.

We now estimate the brilliance of the high-energy ($s > 0.11$) E/L-polarised photon source. The angular divergence of the photon beam is determined by the electron bunch. The total number of photons: $N_\gamma \approx 1.01 \times 10^4$ and 1.76×10^4, is obtained by integrating the angular distributions in Figs. 3(a), (b) respectively over the electron bunch divergence Θ and multiplying the total number of the electrons $N_e = 5 \times 10^6$ in the bunch with a density $n_e \approx 1.33 \times 10^{17}$ cm^{-3} [17], radius $2\lambda_l$ and length $3\lambda_l$ [23], where $\lambda_l = 1$ μm is the laser wavelength. The photon source transverse size is estimated to be the size of the electron bunch and its duration half the sum of the bunch length, $t_e = 3\lambda_l/c = 10$ fs plus laser duration: $t_l = 2\sigma\lambda_l = 26.7$ fs. The photon number in a 0.1% bandwidth (BW) is then obtained by averaging the total number of the photons. We then acquire a prediction for the brilliance for linearly and circularly polarised backgrounds of, respectively, 1.1×10^{21} and 1.9×10^{21} photons/(s mm^2 mrad^2 0.1% BW), which is more than 3 orders of magnitude brighter than recently suggested high energy polarised photon sources [23]. If instead we use FACET II [33] as the electron source, (1 nC of 10 GeV electrons in a bunch volume [10 μm]^3 and density 6.25×10^{18}cm^{-3}), then estimating the angular spread to be $\Theta = 0.2$ mrad, the brilliance would be approximately 100 times higher (1.05×10^{23} and 1.83×10^{23} photons/(s mm^2 mrad^2 0.1% BW), respectively, for the linearly and circularly polarised backgrounds).

This high brilliance and improvement of the polarisation degree on previous suggestions can be explained as follows. First, our scheme exploits photons produced around the edge of the first harmonic, which carries a higher degree of E/L-polarisation than elsewhere in the spectrum, and it is well known that the harmonics (particularly at the Compton edge) cannot be described by the locally-constant-field approximation that is central to numerical simulations employed in other analyses [18–21]. Second, at this lower intensity the angular divergence is extremely narrow and the field-induced angular spread of the electrons is negligible.

The robustness of our scheme is tested by varying the incident angle ϑ_i of the electron beam with a detector directly downstream, set to a fixed acceptance angle $\theta = \Theta$. We see in Fig. 3(d) and Fig. 4 that the high polarisation degree and significant brilliance of the high-energy photons are maintained for a broad range of incident angles. As the bunch incident angle ϑ_i is increased from 0 to 200 mrad, the brilliance decreases less than 5%. One reason for such a small decrease is the relative insensitivity of the energy parameter η to small change in the collision angle from head-on alignment [$\eta \propto \varkappa \cdot p \propto 1 + \cos(\vartheta_i)$]. Further increase of the incident angle to 0.5 rad results in a faster decay of the brilliance.

4. Discussion and conclusion

One way to further improve the brilliance and polarisation degree is to reduce the angular divergence of the electron bunch. If the angular divergence of the electron beam is reduced to the same level of the field-induced angular spread: $\Theta = 2\xi/\gamma_p \approx 0.05$ mrad, the bunch spectra will revert to the single-particle results in Figs. 1 and 2, and the harmonic structure realised. In this way, the brilliance of the high-energy photons $s > 0.11$ can be improved to above 10^{22} photons/(s mm^2 mrad^2 0.1% BW) in Fig. 4, and the corresponding polarisation degree can be improved to about 94% (86%) for a linearly (circularly) polarised background as shown in Fig. 3(d). Furthermore, the photons with different polarisations are angularly separated, and thus a simple angular selection is sufficient to filter pure, highly polarised GeV γ-rays.

In conclusion, we detailed a robust scheme to generate highly polarised GeV γ-rays with ultrahigh brilliance up to 10^{21} photons/(s mm^2 mrad^2 0.1% BW). Our scheme exploits the fact that, starting around the Compton edge, photons are mainly scattered along the electron's propagation axis in one polarisation state. To maximise this effect, a laser pulse with an intermediate intensity should be collided almost head-on with high-energy electrons (~ 10 GeV). (At higher intensities, the photon angular spread becomes larger, and at lower intensities, the probability of scattering is smaller.) A direct calculation from QED is required for these parameters, as they are outside the region of applicability of numerical simulations based on the locally constant field approximation. The brilliance and polarisation degree of the photon source can be further improved by employing electron beams of higher energy and smaller divergence angle and by increasing the spatio-temporal overlap with the colliding laser pulse.

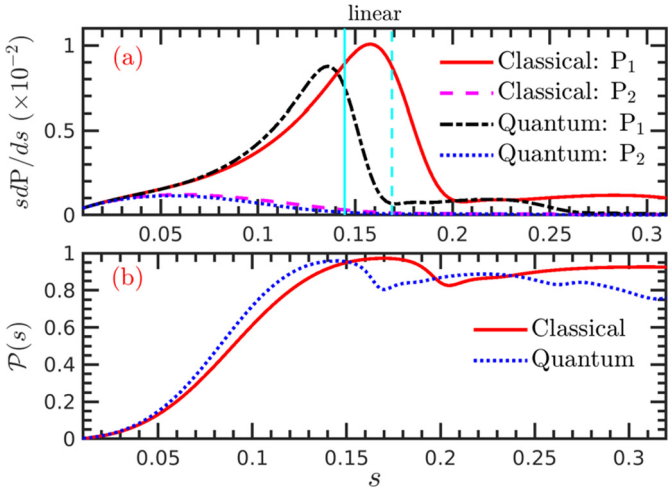

Fig. 5. (a) Energy spectra of the different polarised photons from the exact QED calculations and in the classical limit. (b) The polarisation degree of the E-polarised photon in the QED calculation and the classical limit.

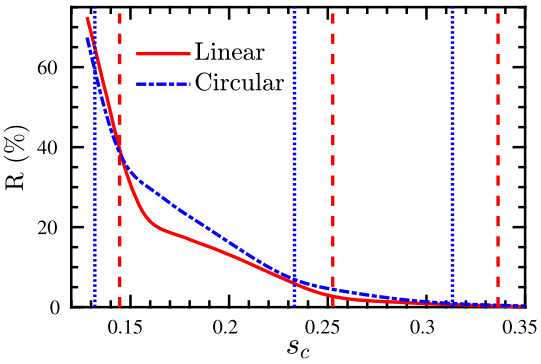

Fig. 6. Ratio of nonlinear contribution to the energy of the highly polarised photons ($s > 0.11$). The vertical dashed (dotted) lines correspond to the bound of the first three harmonics in the linear (circular) backgrounds. The parameters are the same as in Fig. 1.

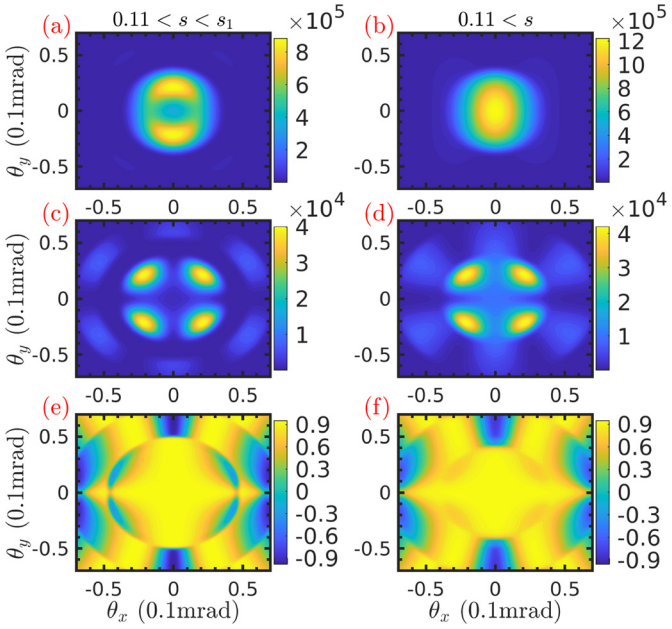

Fig. 7. Linear vs full Compton angular spectra. The cutoff $s > 0.11$ has been applied. $s_1 = 0.144$ is the Compton edge. Left column: high-energy photons from linear Compton ($0.11 < s < s_1$). Right column: high-energy photons from linear and nonlinear Compton ($s > 0.11$). Upper panels: E-polarised photons. Central panels: B-polarised photons. Bottom panels: polarisation degree of the E-polarised photons. The parameters are otherwise the same as in Fig. 1.

Declaration of competing interest

The authors declare that they have no known competing financial interests or personal relationships that could have appeared to influence the work reported in this paper.

Acknowledgements

S. T. and B. K. thank A. Ilderton for a careful reading of the manuscript. They are supported by the UK Engineering and Physical Sciences Research Council, Grant No. EP/S010319/1. H.H. acknowledges the support by the National Natural Science Foundation of China under Grant No. 11774415.

Appendix A

In our suggested scheme, $\eta = 0.095$ and $\xi = 0.5$ have been chosen, and so the corresponding *quantum nonlinearity parameter*, $\chi = \eta\xi \approx 0.05$, which quantifies the electron recoil, is small. In this appendix, we discuss the role of nonlinear and quantum contributions by quantifying them.

A.1. Importance of quantum contributions

The clearest indication of quantum contributions arises when one calculates the position of the harmonics. Let us consider a linearly-polarised background as an example. From QED, we have:

$$s_n^{\mathrm{q}} = \frac{2n\eta}{2n\eta + 1 + \xi^2/2}.$$

If we perform an expansion in $\hbar$ and keep only the leading-order term, then we arrive at the classical expression:

$$s_n^{\mathrm{c}} = \frac{2n\eta}{1 + \xi^2/2}.$$

(this agrees with e.g. the classical analysis in [34]). If one were to use a purely classical approach, the energy of the first, second and third harmonics would be overpredicted by about 17%, 34% and 51%. Therefore, the recoil that the electron experiences due to emission of a photon, is significant in determining the spectrum of produced photons. By performing a classical analysis and comparing it to our QED result in Fig. 5, we can illustrate the contribution of these quantum effects. We note the energy spectrum differs most between the first and second harmonics, which is a key region our scheme exploits to achieve a high polarisation degree.

A.2. Importance of nonlinear contributions

Since we are only in the weakly nonlinear regime of $\xi = 0.5$, one may ask whether the process is a good test of nonlinear QED. We quantify the ratio, R, of nonlinear contributions by calculating the lightfront momentum of the photons above some cutoff, s_c, i.e. $\mathrm{R}(s_c) = \mathcal{E}(s_c)/\mathcal{E}(0.11)$, where $\mathcal{E} = \int_x^\infty (sdP/ds)ds$ and $s_c = 0.11$ is the example filter suggested in the text. As shown in Fig. 6, the nonlinear effect ($s > s_1$) has significant contributions to the energy of the polarised photons: R = 36.9% (59%) for the linear (circular) case.

Another clear indication of the nonlinear contribution originates from the angular spectra. In Fig. 7, we see that the effect of applying an angular cut to the generated GeV-photons, can lead to a different outcome when nonlinear contributions are taken into account.

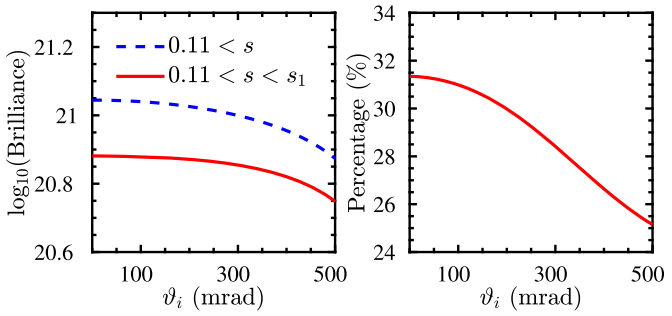

Fig. 8. (a) Brilliance of the E-polarised high-energy photons ($s > 0.11$) from the linear ($s < s_1$) and full ($s > s_1$) Compton process for different incident angle ϑ_i. (b) Percentage of the nonlinear contributions to the total brilliance of the high-energy photon ($s > 0.11$) source. The electron beam angular divergence is $\Theta = 0.2$ mrad. The other parameters are the same as in Fig. 4.

The effect on the predicted brilliance of our nonlinear Compton source is shown in Fig. 8.

Here we see the photons produced by the nonlinear process increase the brilliance by around 30% at a broad range of collision angles.

References

[1] H. Abramowicz, et al., arXiv:1909.00860, 2019.
[2] S. Meuren, P.H. Bucksbaum, N.J. Fisch, F. Fiúza, S. Glenzer, M.J. Hogan, K. Qu, D.A. Reis, G. White, V. Yakimenko, et al., arXiv:2002.10051, 2020.
[3] C. Bula, K.T. McDonald, E.J. Prebys, C. Bamber, S. Boege, T. Kotseroglou, A.C. Melissinos, D.D. Meyerhofer, W. Ragg, D.L. Burke, et al., Phys. Rev. Lett. 76 (1996) 3116, https://link.aps.org/doi/10.1103/PhysRevLett.76.3116.
[4] D.L. Burke, R.C. Field, G. Horton-Smith, J.E. Spencer, D. Walz, S.C. Berridge, W.M. Bugg, K. Shmakov, A.W. Weidemann, C. Bula, et al., Phys. Rev. Lett. 79 (1997) 1626, https://link.aps.org/doi/10.1103/PhysRevLett.79.1626.
[5] C. Bamber, S.J. Boege, T. Koffas, T. Kotseroglou, A.C. Melissinos, D.D. Meyerhofer, D.A. Reis, W. Ragg, C. Bula, K.T. McDonald, et al., Phys. Rev. D 60 (1999) 092004, https://link.aps.org/doi/10.1103/PhysRevD.60.092004.
[6] I.C.E. Turcu, et al., Rom. Rep. Phys. 68 (2016) S145.
[7] B. Shen, Z. Bu, J. Xu, T. Xu, L. Ji, R. Li, Z. Xu, Plasma Phys. Control. Fusion 60 (2018) 044002, https://doi.org/10.1088/1361-6587/aaa7fb.
[8] R.P. Mignani, V. Testa, D. González Caniulef, R. Taverna, R. Turolla, S. Zane, K. Wu, Mon. Not. R. Astron. Soc. (ISSN 0035-8711) 465 (2016) 492, https://doi.org/10.1093/mnras/stw2798, https://academic.oup.com/mnras/article-pdf/465/1/492/8593962/stw2798.pdf.
[9] M.C. Weisskopf, B. Ramsey, S.L. O'Dell, A. Tennant, R. Elsner, P. Soffita, R. Bellazzini, E. Costa, J. Kolodziejczak, V. Kaspi, et al., Results Phys. (ISSN 2211-3797) 6 (2016) 1179, http://www.sciencedirect.com/science/article/pii/S221137971630448X.
[10] B. King, N. Elkina, Phys. Rev. A 94 (2016) 062102, http://link.aps.org/doi/10.1103/PhysRevA.94.062102.
[11] A. Ilderton, M. Marklund, J. Plasma Phys. 82 (2016).
[12] S. Bragin, S. Meuren, C.H. Keitel, A. Di Piazza, Phys. Rev. Lett. 119 (2017) 250403, https://link.aps.org/doi/10.1103/PhysRevLett.119.250403.
[13] A.K. Harding, D. Lai, Rep. Prog. Phys. 69 (2006) 2631, https://doi.org/10.1088/0034-4885/69/9/r03.
[14] B. King, N. Elkina, H. Ruhl, Phys. Rev. A 87 (2013) 042117, https://link.aps.org/doi/10.1103/PhysRevA.87.042117.
[15] Y. Nakamiya, K. Homma, Phys. Rev. D 96 (2017) 053002, https://link.aps.org/doi/10.1103/PhysRevD.96.053002.
[16] K. Horikawa, S. Miyamoto, T. Mochizuki, S. Amano, D. Li, K. Imasaki, Y. Izawa, K. Ogata, S. Chiba, T. Hayakawa, Phys. Lett. B (ISSN 0370-2693) 737 (2014) 109, http://www.sciencedirect.com/science/article/pii/S0370269314005917.
[17] A.J. Gonsalves, K. Nakamura, J. Daniels, C. Benedetti, C. Pieronek, T.C.H. de Raadt, S. Steinke, J.H. Bin, S.S. Bulanov, J. van Tilborg, et al., Phys. Rev. Lett. 122 (2019) 084801, https://link.aps.org/doi/10.1103/PhysRevLett.122.084801.
[18] V.I. Ritus, J. Russ. Laser Res. 6 (1985) 497.
[19] C.N. Harvey, A. Ilderton, B. King, Phys. Rev. A 91 (2015) 013822, https://link.aps.org/doi/10.1103/PhysRevA.91.013822.
[20] A. Di Piazza, M. Tamburini, S. Meuren, C.H. Keitel, Phys. Rev. A 98 (2018) 012134, https://link.aps.org/doi/10.1103/PhysRevA.98.012134.
[21] A. Ilderton, B. King, D. Seipt, Phys. Rev. A 99 (2019) 042121, https://link.aps.org/doi/10.1103/PhysRevA.99.042121.
[22] D. Seipt, B. King, arXiv:2007.11837, 2020.
[23] Y.-F. Li, R. Shaisultanov, Y.-Y. Chen, F. Wan, K.Z. Hatsagortsyan, C.H. Keitel, J.-X. Li, Phys. Rev. Lett. 124 (2020) 014801, https://link.aps.org/doi/10.1103/PhysRevLett.124.014801.
[24] D.Yu. Ivanov, G.L. Kotkin, V.G. Serbo, Eur. Phys. J. C 36 (2004) 127, arXiv:hep-ph/0402139.
[25] D. Seipt, arXiv preprint, arXiv:1701.03692, 2017.
[26] V.N. Baĭer, A.I. Mil'shteĭn, V.M. Strakhovenko, Sov. Phys. JETP 42 (1976) 961.
[27] M. Fukuda, T. Aoki, K. Dobashi, T. Hirose, T. Iimura, Y. Kurihara, T. Okugi, T. Omori, I. Sakai, J. Urakawa, et al., Phys. Rev. Lett. 91 (2003) 164801, https://link.aps.org/doi/10.1103/PhysRevLett.91.164801.
[28] A. Ilderton, B. King, A.J. MacLeod, Phys. Rev. D 100 (2019) 076002, https://link.aps.org/doi/10.1103/PhysRevD.100.076002.
[29] A. Ilderton, B. King, S. Tang, Phys. Lett. B (ISSN 0370-2693) 804 (2020) 135410, http://www.sciencedirect.com/science/article/pii/S0370269320302148.
[30] T. Omori, M. Fukuda, T. Hirose, Y. Kurihara, R. Kuroda, M. Nomura, A. Ohashi, T. Okugi, K. Sakaue, T. Saito, et al., Phys. Rev. Lett. 96 (2006) 114801, https://link.aps.org/doi/10.1103/PhysRevLett.96.114801.
[31] C. Harvey, T. Heinzl, A. Ilderton, Phys. Rev. A 79 (2009) 063407, https://link.aps.org/doi/10.1103/PhysRevA.79.063407.
[32] W.P. Leemans, A.J. Gonsalves, H.-S. Mao, K. Nakamura, C. Benedetti, C.B. Schroeder, C. Tóth, J. Daniels, D.E. Mittelberger, S.S. Bulanov, et al., Phys. Rev. Lett. 113 (2014) 245002, https://link.aps.org/doi/10.1103/PhysRevLett.113.245002.
[33] C. Joshi, E. Adli, W. An, C.E. Clayton, S. Corde, S. Gessner, M.J. Hogan, M. Litos, W. Lu, K.A. Marsh, et al., Plasma Phys. Control. Fusion 60 (2018) 034001, https://doi.org/10.1088/1361-6587/aaa2e3.
[34] B. King, S. Tang, Phys. Rev. A 102 (2020) 022809, https://link.aps.org/doi/10.1103/PhysRevA.102.022809.